Inter-Machine Comparison of Intrinsic Toroidal Rotation

J. E. Rice[1], A. Ince-Cushman[1], J. S. deGrassie[2], L.-G. Eriksson[3], Y. Sakamoto[4], A. Scarabosio[5], A. Bortolon[5], K. H. Burrell[2], C. Fenzi-Bonizec[3], M. J. Greenwald[1], R. J. Groebner[2], G. T. Hoang[3], Y. Koide[4], E. S. Marmar[1], A. Pochelon[5] and Y. Podpaly[1]

[1]Plasma Science and Fusion Center, MIT, Cambridge, MA 02139-4307
[2]General Atomics, La Jolla, CA, USA
[3]EURATOM-CEA, Cadarache, France
[4]Japan Atomic Energy Agency, Naka, Japan
[5]CRPP EPFL, Lausanne, Switzerland

e-mail contact of main author: rice@psfc.mit.edu

Abstract. Parametric scalings of the intrinsic (spontaneous, with no external momentum input) toroidal rotation observed on a large number of tokamaks have been combined with an eye toward revealing the underlying mechanism(s) and extrapolation to future devices. The intrinsic rotation velocity has been found to increase with plasma stored energy or pressure in JET, Alcator C-Mod, Tore Supra, DIII-D, JT-60U and TCV, and to decrease with increasing plasma current in some of these cases. Use of dimensionless parameters has led to a roughly unified scaling with $M_A \propto \beta_N$, although a variety of Mach numbers works fairly well; scalings of the intrinsic rotation velocity with normalized gyro-radius or collisionality show no correlation. Whether this suggests the predominant role of MHD phenomena such as ballooning transport over turbulent processes in driving the rotation remains an open question. For an ITER discharge with $\beta_N = 2.6$, an intrinsic rotation Alfven Mach number of $M_A \sim 0.02$ may be expected from the above deduced scaling, possibly high enough to stabilize resistive wall modes without external momentum input.

1. Introduction and Background

Rotation and velocity shear play important roles in the transition to high confinement mode (H-mode) [1-5], in the formation of internal transport barriers (ITBs) [6,7] and in suppression of resistive wall modes (RWMs) [8,9] in tokamak discharges. In the current generation of tokamaks, rotation is usually provided by the external momentum input from neutral beam injection. In future reactor-grade devices, this may not be available due to the large machine sizes, high densities and the limitations of beam current. For RWM stabilization in certain ITER operational scenarii, it has been estimated that an Alfven Mach number $M_A = 0.02$ will be required [10,11], depending on the velocity profile and normalized pressure, β_N. In a particular ITER case with $n_e = 6.7 \times 10^{19}/m^3$ and $B_T = 5.2$ T, this corresponds to a rotation speed of 200 km/s (30 kRad/s), and it remains an open question whether this level of rotation will be generated from neutral beams. The intrinsic (spontaneous) rotation observed in many tokamaks without external momentum input may, however, provide the necessary velocity. Since the mechanism driving intrinsic rotation is not well understood, and in order to anticipate the level of rotation expected in ITER and other reactor devices, a database of observations on several contemporary machines has been constructed. Intrinsic rotation in L-mode plasmas is often found to be in the counter-current direction, and depends very sensitively on the magnetic configuration [12-14] and in a complicated fashion on other parameters, such as the density, plasma current and ion temperature [13-15]. While the study of intrinsic rotation in L-mode discharges is of interest in its own right (e.g. for its relation to the H-mode power threshold [13-14]), these plasmas will not be considered here, since most ignition scenarii in future devices require H-mode confinement. The intrinsic toroidal rotation in H-mode or in other enhanced confinement regimes, which will be the main subject of this

paper, is generally in the co-current direction. Co-current intrinsic rotation has been observed on many devices and produced with a wide variety of techniques, demonstrating its fundamental nature. Substantial rotation velocities have been obtained in ion cyclotron range of frequencies (ICRF) heated plasmas on JET [16,17], Alcator C-Mod [18,19,13] and Tore Supra [20-22]. Co-current rotation has been seen in Ohmic H-mode discharges in COMPASS-D [23], Alcator C-Mod [19,24,25] and DIII-D [26,27]. Similarly, co-current rotation has been observed at the edge of electron cyclotron heated (ECH) H-mode plasmas on DIII-D [26,27], on JT-60U [28] with a combination of lower hybrid (LH) waves and ECH, and in TCV with core ECH. Velocities up to 130 km/s have been measured in H-mode plasmas, without external momentum input. A common feature of all of these observations is a strong correlation between the toroidal rotation velocity and the plasma pressure or stored energy [16,18,19,24,25,29,21,22,27,28]. In experiments which can operate with a large range of plasma current, the rotation velocity is found to be inversely proportional to I_p [19,25,29,22,27]. The coefficient of this scaling is different on different devices, and probably includes some machine size scaling information.

The goal of this paper is to examine and compare the scalings of intrinsic rotation from individual devices in enhanced confinement regimes and to develop a global scaling with dimensionless variables, with an eye toward extrapolation to ITER and guiding a theoretical explanation. In the next section, observations of intrinsic rotation on various tokamaks are summarized, in Section 3, the results of dimensionless scalings are presented and in Section 4 the connection with theory is outlined.

2. Summary of Instinsic Rotation Observations

Co-current spontaneous rotation during H-mode operation was first observed in JET ICRF heated plasmas [16], where a strong correlation was found between the local angular momentum density and the ion pressure for low D_α discharges (Fig. 10 of Ref.[16]). Intrinsic rotation velocities as high as 60 km/s were measured using passive x-ray spectroscopy. Spontaneous rotation in ICRF heated H-mode plasmas has been studied extensively in Alcator C-Mod [18,19,29,30,13,31], with velocities up to 130 km/s (thermal ion Mach number M_i = 0.3) measured in discharges with no direct momentum input, also utilizing passive x-ray spectroscopy. The main C-Mod results are summarized as follows: the rotation during H-mode is in the co-current direction, changing direction, but remaining co-current when the current direction is reversed. The change in the rotation velocity between L- and H-mode increases with the change in the plasma stored energy during ICRF heating (Fig.1 of Ref.[19]) and decreases with the magnitude of the plasma current (Fig.2 of Ref.[29]); the time history of the rotation velocity tracks the time evolution of the plasma stored energy, W_p, and not the electron density or ion temperature independently. The intrinsic rotation is seen to propagate in from the plasma boundary following the H-mode transition, with a momentum confinement time similar to the energy confinement time [30,13], and highly anomalous compared to neo-classical theory. The rotation velocity profiles are flat in EDA H-mode and centrally peaked in ELM-free H-mode, implying the presence of an inward momentum pinch in the latter case. In Tore Supra, strong co-current toroidal rotation, with velocities reaching 80 km/s, has similarly been observed in ICRF heated enhanced confinement regimes [20-22], also using passive x-ray spectroscopy. A scaling similar to the C-Mod results, with the change in the rotation velocity increasing with the change in the stored energy normalized to the plasma current, has been observed (Fig.3 of Ref.[22]). In this case the slope of a line through the data points is a little over a factor of two less than in C-Mod, and this presumably contains some machine size

scaling information. The best correlation of the intrinsic rotation velocity in Tore Supra is with the ion pressure.

Co-current toroidal rotation in Ohmic H-mode discharges was first documented in COMPASS-D [23]. Spontaneous rotation in Ohmic H-mode plasmas has been studied extensively in C-Mod [24,25], and the observations are essentially identical to those in ICRF H-modes in terms of the scaling with W_p/I_p (Fig.4 of Ref.[25] and Fig.2 of Ref.[29]). This is suggestive of a common driving mechanism not involving energetic ions [31]. Co-current intrinsic rotation during Ohmic H-modes has also been observed in DIII-D [26,27] and TCV, using charge exchange recombination spectroscopy, with heating neutral beam blips in the former case and a diagnostic neutral beam in the latter. The rotation velocity profiles during Ohmic H-modes in C-Mod and DIII-D are flat.

Co-current intrinsic rotation has also been observed in ECH discharges. In DIII-D ECH H-modes [26,27], rotation velocities as high as 30 km/s at r/a = 0.8 have been measured. The profile shape depends on the ECH resonance location, with hollow profiles occurring under on-axis heating; no velocity increase in the plasma center over the L-mode background value is seen. Off-axis ECH leads to relatively flat velocity profiles. Regardless of the resonance location, the maximum co-current velocity increase is near r/a = 0.8. A scaling of the rotation velocity near r/a = 0.8 as a function of the plasma stored energy normalized to the plasma current in DIII-D ECH and Ohmic H-modes shows a very similar scaling (Fig. 3 of Ref.[27]) to those seen in C-Mod and Tore Supra, suggesting a fundamental connection between observations of intrinsic rotation, regardless of the production technique. A slightly better fit to the DIII-D data was found multiplying W_p/I_p by $T_e(0)/T_i(0)$. The slope of the fit was lower than that found in C-Mod and Tore Supra. Strong co-current intrinsic rotation, with velocities as high as 120 km/s, has been observed in JT-60U plasmas with a combination of LH and ECH [28], utilizing the very beginning of the heating neutral beam pulse. These discharges were at low electron density ($n_e = 4 \times 10^{18}/m^3$ and $T_e \gg T_i$), had electron temperature ITBs and exhibited slightly peaked velocity profiles. Similar to the scalings described above, there was a strong correlation between the rotation velocity and the electron pressure. Co-current spontaneous rotation has also been observed in TCV ECH H-mode [32] plasmas, with velocities up to 35 km/s.

The observations represented here are from diverse plasma conditions using a variety of techniques (dominant ion heating, dominant electron heating, varying degrees of electron-ion coupling, different levels of toroidal field ripple, etc.), yet there are remarkable similarities in the observations. The results of the intrinsic rotation observations from the six different devices outlined above represents a range of minor radius from 0.21 m (C-Mod) to 1.25 m (JET), major radius from 0.67 m (C-Mod) to 3.4 m (JT-60U), B_T from 1.4 T (TCV) to 5.4 T (C-Mod) and I_p from 0.3 MA (TCV) to 3.0 MA (JET), covering roughly a factor of five in these parameters. The range of the maximum intrinsic V_ϕ observed varies from 30 km/s (20 kRad/s in DIII-D) to 130 km/s (200 kRad/s in C-Mod), and W_p from 0.04 MJ (TCV) to 4 MJ (JET). Obviously the stored energy has an important contribution from the plasma volume. One goal of this paper is to predict the level of intrinsic rotation expected in certain ITER operational schemes. In a first attempt to combine the results from different devices, the scalings of the impurity toroidal rotation velocity $\Delta V_\phi \propto \Delta W_p/I_p$ from C-Mod (Fig.2 of Ref.[29]), Tore Supra (Fig.3 of Ref.[22]) and DIII-D (Fig.3 of Ref.[27]) have been reproduced on the same scale in Fig.1. While the scalings are all similar, the best fit slopes are in the

ratios of 100:43:7; this presumably contains some machine size scaling information, and will be explored in the next section.
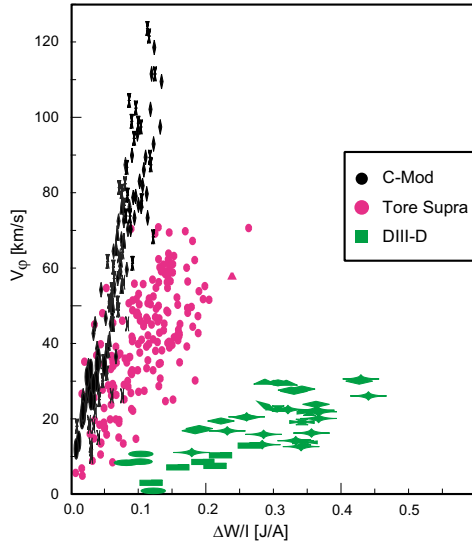

Fig.1 The intrinsic rotation velocity (the difference between the L-mode velocity and the enhanced confinement value) as a function of the change in the stored energy normalized to the plasma current for Alcator C-Mod (black), Tore Supra (red) and DIII-D (green).
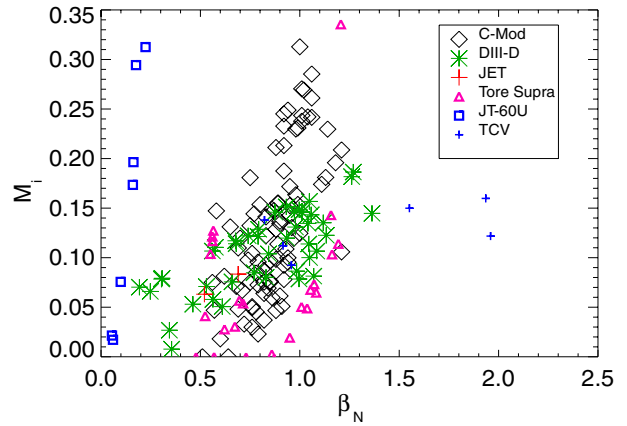

Fig.2 The ion thermal Mach number as a function of β_N for C-Mod (black diamonds), DIII-D (green asterisks), JET (red + signs), JT-60U (blue squares), TCV (small blue + signs) and Tore Supra (red triangles).

3. Scalings of Intrinsic Rotation with Dimensionless Parameters

In order to unify the rotation measurements on all of these devices, the approach of utilizing dimensionless variables has been followed. For the rotation velocity, several normalizations have been considered, including the ratio of the impurity toroidal velocity to the ion thermal velocity, $M_i \equiv V_\phi/v_i$, and to the Alfven speed, $M_A \equiv V_\phi/C_A$. The plasma stored energy (or pressure) normalized to the plasma current is contained in the commonly used normalized plasma pressure, $\beta_N \equiv \beta_T\, a\, B_T/I_p$, with $\beta_T \equiv 2\mu_0 <P>/B_T^2$ ($<P>$ is the average pressure), the minor radius a in m, the toroidal magnetic field B_T in T and the plasma current I_p in MA. This is essentially W_p/I_p with a geometric factor depending on the machine size and $1/B_T$. An example of a dimensionless scaling is demonstrated in Fig.2 in which is shown M_i as a function of β_N for the six machines C-Mod, DIII-D, JT-60U, JET, TCV and Tore Supra. Most of the points follow a similar trend, with M_i increasing as β_N, and all machines except JT-60U are overlain. In contrast to Fig.1, this suggests that the dimensionless approach unifies the results from different machines. For JT-60U, these particular discharges were at low electron density, had narrow ITBs, very low β and $T_e >> T_i$, so were quite different from the plasmas on the other devices. The scaling with M_A as a function of β_N is shown in Fig.3, which brings the points in a little tighter and does a much better job incorporating JT-60U. This simple scaling brings all of the various results from all devices into accord, on the same scale. Strictly speaking, β_N isn't dimensionless (units of % Tm/MA) but can be made so by dividing by μ_0: $\beta_N' \equiv \beta_N/40\pi$ is truly dimensionless. The same plot as Fig.3 but with β_N' is depicted in Fig.4, and the best fit through the data points has a slope of around 1.
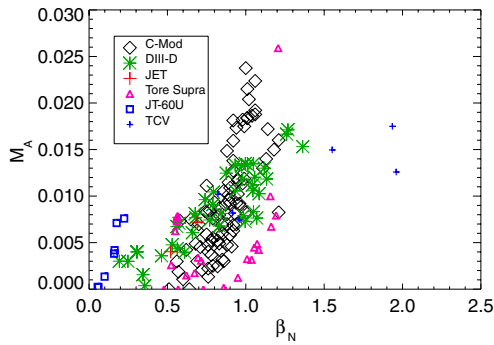
Fig.3 The Alfven Mach number as a function of β_N, with the same legend as Fig. 2.
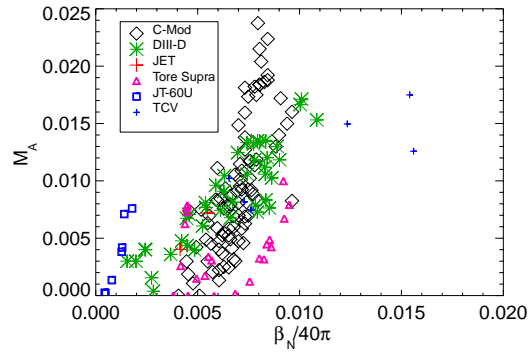

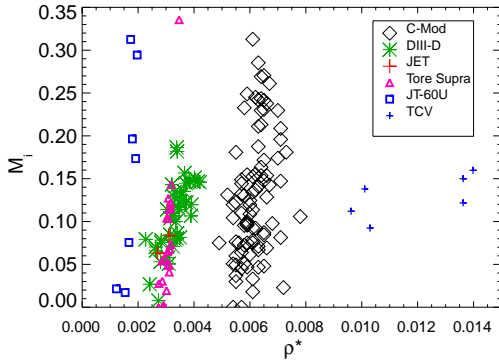*Fig.4   The Alfven Mach number as a function of $\beta_N/40\pi$, with the same legend as Fig. 2..*

Fig.5 The ion thermal Mach number as a function of ρ^*, with the same legend as Fig. 2.
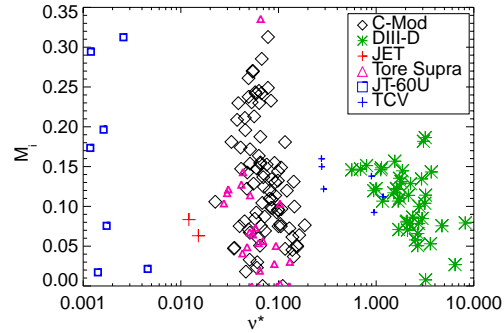

Fig.6 The ion thermal Mach number as a function of ν^*, with the same legend as Fig. 2.

Scalings of the Mach numbers with ρ^*, the normalized gyro-radius, shown in Fig.5, do not exhibit any clear trends, either for observations on an individual device or for an inter-machine comparison. The square root of the temperature contained in ρ^* is roughly the same on all devices, so the different machines are sorted in vertical strips in ρ^* according to the minor radius and toroidal magnetic field. This implies that ρ^* is not important in generating or regulating intrinsic rotation. For typical ITER operation, ρ^* will be in the neighborhood of 1.5×10^{-3}, but since there is no predictive capability from Fig.5, no estimate can be made for the expected level of rotation. Similarly, scalings of the Mach numbers with the collisionality ν^* fail to show any correlation, as demonstrated in Fig.6. Again, the rotation velocities from the different devices appear in vertical strips, and the implication is that collisionality is not a relevant player in driving or governing intrinsic rotation.

Based on the general trend in Fig.2, a ion thermal Mach number M_i in the neighborhood of 0.3 may be extrapolated for an ITER discharge with $\beta_N = 2.6$, and for $T_i = 12$ keV, this corresponds to an intrinsic rotation velocity of 250 km/s or 40 kRad/s. For a conservative extrapolation of the scaling in Fig. 3, an Alfven Mach number M_A of 0.02 for an ITER discharge at $\beta_N = 2.6$ would be reasonable, probably high enough to stabilize RWMs [10].

4. Comparison with Theory

Several approaches toward an explanation of the observed intrinsic/spontaneous rotation have been undertaken. An obvious starting point is a comparison with the predictions of neo-classical theory. Using a moment formulation [33] in conjunction with radial force balance,

$$V_\phi \quad = \quad 1/B_\theta \{E_r - (\partial P_i/\partial r)/en_i + \partial T_i/\partial r \, (K_1 + 3/2 \, K_2)/e\} \tag{1}.$$

Here V_ϕ is the impurity toroidal rotation velocity, B_θ is the poloidal magnetic field, E_r is the radial electric field, e is the electric charge, n_i, P_i and T_i are the ion density, pressure and temperature, respectively, and K_1 and K_2 are functions evaluated for all collisionality regimes in the appendix of Ref.[34]. This expression captures some of the general features of the observed intrinsic rotation velocity scaling shown in Fig.1: the plasma pressure or stored energy is widely found to increase with the pedestal pressure gradient (second term in Eq.1), and the plasma current is directly related to the poloidal magnetic field. Unfortunately, the radial electric field (first term in Eq.1) is rarely measured directly (in practice it is inferred from the routinely available rotation velocity [35]) and remains largely an unknown, yet dominant, parameter in Eq.(1). Furthermore, the standard neo-classical theory may not be valid at the edge of some H-mode discharges because the normal ordering, that the ion gyro-radius is small compared to the ion temperature gradient scale length, is violated. The sub-neo-classical theory [36,37] properly treats this situation, and has the added benefit of providing E_r from an ambipolarity constraint. The predicted toroidal rotation velocity is in reasonable quantitative agreement with observations on C-Mod [38] under certain operating conditions [31]. However, a fundamental problem with neo-classical and sub-neo-classical theory is that the momentum diffusivity [39] (viscosity) is orders of magnitude smaller than that observed in experiments [30 and references therein].

Since the early observations of intrinsic rotation were in ICRF heated discharges, it was natural to consider models based on energetic ion orbit shift mechanisms [40-43]. However, the similarity of the intrinsic rotation observed in ICRF, ECH and purely Ohmic plasmas suggests that it is not due to ICRF wave or fast ion orbit effects. The prediction of reversal of the rotation direction with high magnetic field side off-axis ICRF absorption [41,43] has not been observed in the C-Mod experiments [31]. Energetic ion orbit effects have also been ruled out as a source of rotation in JET [16] and Tore Supra [21].

An alternative approach to explain the spontaneous generation of rotation is based on turbulence [44]. Fluctuation induced toroidal stress [45] can give rise to toroidal rotation where the direction of the rotation depends upon the mode frequency spectrum, and may explain the reversal of the observed rotation in going from L- to H-mode. The calculated magnitude of the rotation is a function of the level of the turbulence, and a quantitative comparison with experimental results is not yet possible. A comparison of predicted velocity profile shapes in C-Mod plasmas has produced mixed results [31]. A similar model [46] of electrostatic modes driven by the ion pressure gradient is in qualitative agreement with many of the features observed in the C-Mod experiment: direction of rotation in L- and H-mode, scaling with W_p/I_p in H-mode and the drop in the rotation observed in ITB plasmas. However, there are no quantitative predictions about the magnitude of the rotation or the size of the momentum diffusivity for further comparison with the experimental results. Furthermore,

these turbulence based theories do not provide a scaling of the turbulence levels with plasma parameters which would allow a direct comparison with the results of Figs.2-4.

It has recently been suggested [47] that the blob transport at the edge of C-Mod plasmas could possibly drive the rotation if the blobs are leaving the plasma at some toroidal angle. Whether the total momentum of blobs leaving the plasma edge is enough to spin the plasma in the opposite direction remains an open question for future work.

5. Discussion and Conclusions

Given the very limited success of the above theoretical approaches in explaining the mechanism driving intrinsic rotation, the empirical scaling has been examined in order to provide hints of the fundamental cause. The scaling $M_A = \beta_N/40\pi$ is suggestive of an underlying MHD mechanism, although perhaps not a direct effect. The character of the transport in the plasma edge in C-Mod is ballooning in nature [14], driving edge flows along field lines from the low to high field regions, and the rotation in the plasma center is well known to respond to changes at the edge (coupled by the momentum diffusivity [30,13]). This is certainly consistent with an MHD process governing intrinsic rotation, although drift Alfven resistive ballooning theory doesn't use MHD ordering. The ballooning parameter [48], $q^2R\beta_T/L_P$ (where L_P is the pressure gradient scale length), captures some of the features of the observed scaling, notably a common factor of $qR\beta_T$. A direct comparison with the ballooning parameter (as in Figs.2-8) is not yet possible since the edge pressure gradient scale length is not routinely measured on the six devices compared above. The role of the q profile in intrinsic rotation is still under investigation. Since the intrinsic rotation is independent of $\rho*$ and $\nu*$, the implication is that certain types of turbulence are not involved in its generation or regulation. Regardless of the underlying cause, the intrinsic rotation scaling developed above extrapolates to a substantial velocity for ITER, and coupled with the variety of velocity profile shapes (peaked on C-Mod, flat on C-Mod and JT-60U, hollow on DIII-D) observed using different techniques, the prospects for rotation control on ITER look encouraging. Hopefully guided by this apparent universal scaling, a better theoretical understanding of spontaneous rotation will emerge.

6. Acknowledgements

References

[1]   K.C.Shaing and E.C.Crume, Phys. Rev. Lett. **63** (1989) 2369.
[2]   H.Biglari et al., Phys. Fluids **B2** (1990) 1.
[3]   R.J.Groebner et al., Phys. Rev. Lett. **64** (1990) 3015.
[4]   K.Ida et al., Phys. Rev. Lett. **65** (1990) 1364.
[5]   P.W.Terry, Rev. Mod. Phys. **72** (2000) 109.
[6]   T.S.Hahm, Phys. Plasmas **1** (1994) 2940.
[7]   K.Burrell, Phys. Plasmas **4** (1997) 1499.
[8]   E.J.Strait et al., Phys. Rev. Lett. **74** (1994) 2483.
[9]   L.-J.Zheng, M.Kotschenreuther and M.S.Chu, Phys. Rev. Lett. **95** (2005) 255003.

[10] A.R.Polevoi et al., Proc. 19th IAEA Conf. Lyon 2002, IAEA-CN-94-CT/P-08.

[11] Yueqiang Liu et al., Nucl. Fusion **44** (2004) 232.

[12] J.E.Rice et al., Nucl. Fusion **37** (1997) 421, and references therein.

[13] J.E.Rice et al., Nucl. Fusion **44** (2004) 379.

[14] B.LaBombard et al., Nucl. Fusion **44** (2004) 1047.

[15] A.Scarabosio et al., Plasma Phys. Contr. Fusion **48** (2006) 663.

[16] L.-G.Eriksson et al., Plasma Phys. Contr. Fusion **39** (1997) 27.

[17] J.-M.Noterdaeme et al., Nucl. Fusion **43** (2003) 274.

[18] J.E.Rice et al., Nucl. Fusion **38** (1998) 75.

[19] J.E.Rice et al., Nucl. Fusion **39** (1999) 1175.

[20] G.T.Hoang et al., Nucl. Fusion **40** (2000) 913.

[21] L.-G.Eriksson et al., Nucl. Fusion **41** (2001) 91.

[22] S.Assas et al., 30th European Physical Society Conference on Plasma Physics and Controlled Fusion, St. Petersburg, Russia, 7-11 July 2003, ECA Vol. {\bf 27A} P-1.138

[23] I.H. Coffey, R. Barnsley, F.P. Keenan {\it et al.}, in Proc. of the 11th Colloquium on UV and X-ray Spectroscopy of Astrophysical and Laboratory Plasmas, Nagoya, Japan, 1995, p.431, Frontiers Science Series No.15, Universal Academy Press, Tokyo, 1996

[24] I.H.Hutchinson et al., Phys. Rev. Lett. **84** (2000) 3330.

[25] J.E.Rice et al., Phys. Plasmas **7** (2000) 1825.

[26] J.S.deGrassie et al., Phys. Plasmas **11** (2004) 4323.

[27] J.S.deGrassie et al., Proc. 20th IAEA Conf. Vilamoura 2004, IAEA-CN-116-EX/6-4Rb.

[28] Y. Sakamoto et al., 10th IAEA TCM, St. Petersburg, Russia, 28 Sept. 2005

[29] J.E.Rice et al., Nucl. Fusion **41** (2001) 277.

[30] W.D.Lee et al., Phys. Rev. Lett. **91** (2003) 205003.

[31] J.E.Rice et al., Phys. Plasmas **11** (2004) 2427.

[32] L. Porte et al., 'Vertical Launch Third Harmonic Electron Cyclotron Heating of H-mode on TCV', submitted to Plasma Phys. Control. Fusion (2006)

[33] S.P.Hirshman and D.J.Sigmar, Nucl. Fusion **21** (1981) 1079.

[34] Y.B.Kim et al., Phys. Fluids **B3** (1991) 2050.

[35] K.Ida, Plasma Phys. Contr. Fusion **40** (1998) 1429.

[36] A.L.Rogister, Phys. Plasmas **6** (1999) 200.

[37] H.A.Claassen, H.Gerhauser, A.Rogister and C.Yarim, Phys. Plasmas **7**, (2000) 3699.

[38] A.L.Rogister et al., Nucl. Fusion **42** (2002) 1144.

[39] F.L.Hinton and S.K.Wong, Phys. Fluids **28** (1985) 3082.

[40] C.S.Chang et al., Phys. Plasmas **6** (1999) 1969.

[41] F.W.Perkins et al., Phys. Plasmas **8** (2001) 2181.

[42] V.S.Chan et al., Phys. Plasmas **9** (2002) 501.

[43] L.-G.Eriksson and F.Porcelli, Nucl. Fusion **42** (2002) 959.

[44] P.H.Diamond et al., Proc. 15th IAEA Conf. Seville 1994, IAEA-CN-60/D-13.

[45] K.C.Shaing, Phys. Rev. Lett. **86** (2001) 640.

[46] B.Coppi, Nucl. Fusion **42** (2002) 1.

[47] J.R.Myra et al., Proc. of the 19th US TTF Meeting, Myrtle Beach, S.C., Apr. 2006

[48] J.W.Connor et al., Phys. Rev. Lett. **40** (1978) 396.